CERN–TH/99–118
PM/98–38
RU–98–45
hep-ph/9905443
May 24, 1999

Higgs– and Slepton–Strahlung at Hadron Colliders

Francesca Borzumati[a], Jean-Loïc Kneur[b], and Nir Polonsky[c]
[a] *Theory Division, CERN, CH-1211 Geneva 23, Switzerland*
[b] *Laboratoire de Physique Mathématique et Théorique, Université de Montpellier II, F–34095 Montpellier Cedex 5, France*
[c] *Department of Physics and Astronomy, Rutgers University, Piscataway, NJ 08854-8019, USA*

Abstract

It is shown that the radiation of a charged Higgs boson off a third-generation quark (charged-Higgs–strahlung) provides an important channel for the discovery of the charged Higgs at hadron colliders. Equivalently, in supersymmetric models with explicit lepton-number (R–parity) violation, sleptons may also be produced in association with quarks (slepton–strahlung). Higgs– and slepton–strahlung production cross sections are given for both the Tevatron and the LHC. The LHC cross sections imply that heavy $\mathcal{O}$(TeV) charged Higgs bosons can be produced via charged-Higgs–strahlung and that strahlung production of charged sleptons is possible even for small R–parity violating couplings. The possible discovery of sleptons through this channel offers a surprising handle on models of neutrino masses.

I. INTRODUCTION

While the LEP experiments reach their final phases, the upgraded Tevatron ($\sqrt{s} = 2$ TeV) at FNAL and the CERN Large Hadron Collider (LHC) ($\sqrt{s} = 14\,\text{TeV}$) will provide the next front in searches for particles associated with physics beyond the Standard Model (SM). In particular, since LEP cannot probe masses significantly above the 100 GeV mark, the probe of heavier particles will remain the task of these two hadronic machines. Sufficient production cross sections at these colliders, however, may be difficult to achieve if the new particles carry only weak charges. Effective couplings of these particles to (initial) gluons may be induced at the quantum level, but they suffer from loop suppression and hence, are generically small. Sufficiently large and measurable production cross sections require either some enhancement of the radiative gluonic couplings or an alternative production mechanism.

In the case of the Higgs bosons present in supersymmetric models, as well as non-supersymmetric two Higgs doublet models, there exist two potentially large parameters which can partially compensate for the otherwise small couplings: the intrinsically large t-quark Yukawa coupling and the ratio of vacuum expectation values (*vev*s) of the two neutral Higgs bosons $\tan\beta = v_2/v_1$, which is constrained from above to be $\lesssim 60$ by the perturbativity of Yukawa couplings. They may (*i*) enhance the radiatively induced gluonic coupling of the neutral Higgs, in proportion to the t-quark Yukawa coupling, leading to production via $gg \to H^0$ [1]; (*ii*) sufficiently increase the rate for the decay of the t-quark into a (light) charged Higgs boson, $t \to H^+ b$ [2–5]; or (*iii*) enhance the Higgs–strahlung associate production through the $2 \to 3$ partonic processes gg, $qq \to qqH^0$, $qq'H^\pm$ [6–10], through the $2 \to 2$ ones $qg \to qH^0$, $q'H^\pm$ [9,11,12], and through the $2 \to 1$ process $\bar{b}b \to H^0$ [9,10]. (For an overview, see, for example, Ref. [13].)

From charge conservation, a radiatively induced gluonic coupling cannot lead, at the level of an elementary process, to the production of only one charged Higgs. Hence, one needs to consider either the single production from t-quark decays or the production in association with quarks – which is referred to as Higgs–strahlung. Production in association with gauge bosons WH^0/ZH^0, $W^\pm H^\mp$, and in supersymmetric models, in association with squarks, are also possible. The former mechanism, however, leads to subleading cross sections which are difficult to observe [14,15]. The latter [16–18], is more model-dependent and will not be considered here. The production mechanisms with one single Higgs (and quarks) in the final state, or "single production", are kinematically in advantage in comparison to pair production mechanisms. These include (*a*) the Drell–Yan process $q\bar{q} \to H^+H^-$, which is suppressed by weak couplings and, at the LHC, by the low quark luminosities (relative to the gluon one); and (*b*) effective gluonic couplings, which are now allowed by charge invariance, $gg \to H^+H^-$ [19]. Pair production, therefore, does not allow discovery of the charged Higgs at the Tevatron. At the LHC, it provides a limited discovery reach of the charged Higgs in a non-supersymmetric two Higgs doublet model [19], but it may become more competitive in supersymmetry where additional contribution to the effective gluonic couplings arise [20,21].

Our focus here is on the single production of a charged Higgs boson. Single production from t-quark decays plays the most important role when kinematically allowed, that is for $m_{H^\pm} < m_t - m_b$, and was studied extensively by various authors [4]. The charged-Higgs–

strahlung in the $2 \to 3$ channels gg, $qq \to tH^-\bar{b}$ encompasses the resonant production of a pair $t\bar{t}$ followed by the decay $\bar{t} \to H^-\bar{b}$ in the same kinematical region $m_{H^\pm} < m_t - m_b$ and, in addition, provides the intrinsically off-shell associate production of $H^\pm$ beyond this kinematical limit, throughout all possible ranges of $m_{H^\pm}$. Strahlung from the $2 \to 2$ channel $gb \to tH^-$ is also possible, since the b-quark is obtained from the proton via a gluon. Therefore, both types of partonic processes, the $2 \to 3$ and the $2 \to 2$, give rise to inclusive processes which are formally of the same order in an α_s expansion. Note that away from the resonance region, H^- decays dominantly into $\bar{t}b$, and the t-quark into W^+b. Thus, the $2 \to 3$ processes gg, $qq \to tH^-\bar{b}$ give rise to four b-quarks in the final state, whereas only three b's are produced in the $2 \to 2$ process $gb \to tH^-$. Both elementary processes contribute to the inclusive production of a single charged Higgs at hadron colliders, when at most three b-quarks are tagged and used to identify the final particle configuration. If four b's can be detected, it is possible to measure each cross section separately. Otherwise, the two elementary processes have to be properly combined into an inclusive cross section, avoiding double counting of the contributions coming from $gb \to tH^-$ and from $gg \to tH^-\bar{b}$, when one of the two gluons produces a $b\bar{b}$ pair collinear to the initial proton (or antiproton). Since identification and detection issues will not be discussed here, both the individual-channel and inclusive cross sections will be given below.

The charged-Higgs production cross sections are calculated and illustrated for the upgraded Tevatron and the LHC in Section II, where all relevant issues are discussed in detail. Attention is given to the prospects of discovery at the Tevatron, which may constrain $m_{H^\pm}$ beyond the kinematical limit $m_{H^\pm} < m_t - m_b$. It is found that a charged Higgs as heavy as $\mathcal{O}(\mathrm{T}eV)$ may be produced via the strahlung processes at the LHC. The results shown are valid for the charged Higgs of supersymmetric and non-supersymmetric two Higgs doublet models. The charged-Higgs decay modes, however, may differ in the two classes of models if $m_{H^\pm}$ is sufficiently large [3,2].

For reference, the indirect lower limit on $m_{H^\pm}$ coming from the measurement of the inclusive decay $b \to s\gamma$ amounts (at present) only to $\sim 165\,\mathrm{GeV}$ [22] in non-supersymmetric two Higgs doublet models. No substantial limit exists for charged Higgs in supersymmetric models, when supersymmetric partners can be exchanged in the loop mediating the $b \to s\gamma$ decay. Direct lower bounds on $m_{H^\pm}$ are given by collider searches at LEPII and at the Tevatron. The LEPII bound, $m_{H^\pm} \gtrsim 54\,\mathrm{GeV}$ [23] at $\sqrt{s} = 130\,\mathrm{GeV}$ ($m_{H^\pm} \gtrsim 68\,\mathrm{GeV}$ at higher energy runs [13]), applies to the case of a charged Higgs boson present in two Higgs doublet models. The Tevatron searches give combined (and currently modest) bounds in the $m_{H^\pm}$–$\tan\beta$ plane for supersymmetric and non-supersymmetric charged Higgs bosons. Both searches have been critically discussed in Ref. [2]. Conservatively, all results presented in this paper are shown for $m_{H^\pm} \gtrsim 45\,\mathrm{GeV}$, the model-independent limit extracted from the measurement of the Z width.

In supersymmetric models in which R–parity and lepton number are not conserved, the hypercharge $Y = -1$ Higgs and slepton fields are not distinguished by any quantum numbers and could interact in a similar way. Thus, in these models, sleptons can be produced via slepton–strahlung just as the (charged) Higgs. The relevant Yukawa couplings, i.e. the slepton–fermion–fermion couplings, are subject to various low-energy constraints but are otherwise arbitrary since they do not relate to fermion masses (once the two Higgs doublets

are identified as those whose neutral components are aligned along the two large *vevs*). They are however related to radiative neutrino masses, as explained below, and therefore measurements of lepton number violating operators from slepton production provide a unique and important window on this class of models for neutrino masses. The associate production cross section for the charged sleptons is presented for both the Tevatron and the LHC experiments in Section III. It is shown that charged sleptons can be produced in abundance for R–parity violating couplings as small as 0.01. Relations and possible lessons to models of neutrino masses are also demonstrated in Section III. We also comment on the case of the neutral sleptons, the sneutrinos $\tilde{\nu}$, which is complicated by the presence of the gluon fusion channel $gg \to \tilde{\nu}$.

Results and discussions of the potential impact of these strahlung channels on future searches are summarized in Section IV, where we also comment on the possibility that both charged-Higgs and slepton–strahlung channels are present.

All calculations are done at the leading order in QCD. Higher order corrections may be important, as it was shown in the case of associate production of the neutral Higgs [24]. Their inclusion is called upon, but it is left for future work.

II. CHARGED-HIGGS–STRAHLUNG

The charged Higgs boson interacts with quarks according to the lagrangian

$$\mathcal{L} \;=\; \frac{g}{\sqrt{2}} \left\{ \left(\frac{m_{di}}{M_W} \tan\beta \right) V_{ji}\, \overline{u}_{Lj}\, d_{Ri} + \left(\frac{m_{ui}}{M_W} \cot\beta \right) V^*_{ji}\, \overline{u}_{Ri}\, d_{Lj} \right\} H^+ + \text{h.c.}\,, \tag{1}$$

where the standard notations for the SU(2) coupling g, the up- and down-quarks u_i and d_i of a generation i, and for the Cabibbo–Kobayashi–Maskawa (CKM) matrix V are followed. Hereafter, all intergenerational mixing terms are neglected, as well as all Yukawa couplings other than those for the t- and b-quarks, which have respectively strength $h_t \simeq g m_t/(\sqrt{2} M_W \sin\beta) \simeq 1/\sin\beta$ and $h_b \simeq g m_b/(\sqrt{2} M_W \cos\beta) \simeq 0.017 \tan\beta$. Since all calculations are done to leading order, model-dependent radiative corrections to these relations [4,25] are also omitted. They could, however, be large and play an important role (at the order in perturbation theory at which they must be included) by smearing the $\tan\beta$ dependence of the $H^\pm$-production cross sections.

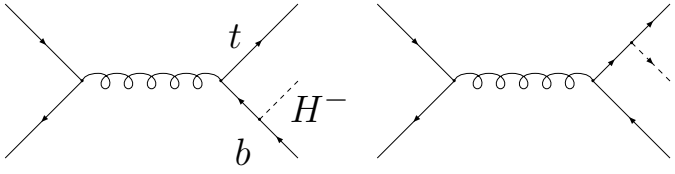

FIG. 1. Diagrams contributing to $p\bar{p}\,(pp) \to tH^-(\bar{b})X$ through an elementary quark-initiated $2 \to 3$ process.

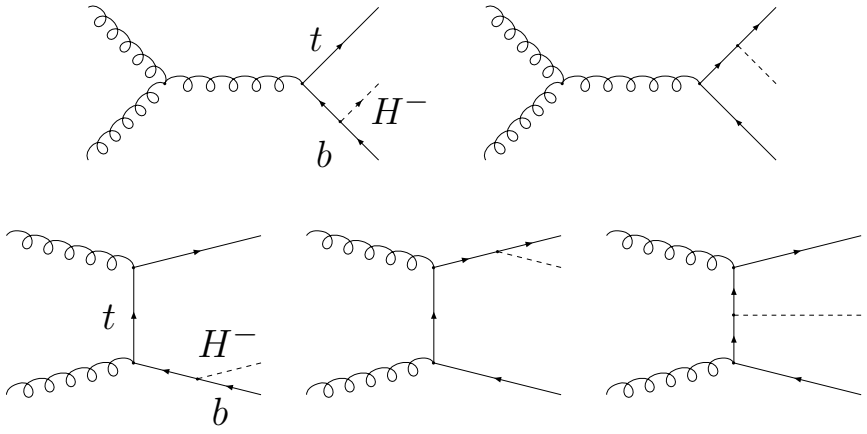

FIG. 2. Diagrams contributing to $p\bar{p}\,(pp) \to tH^-(\bar{b})X$ through an elementary gluon-initiated $2 \to 3$ process.

A. The $2 \to 3$ process: cross section calculation

Quarks produced in quark or gluon collisions can radiate a Higgs boson leading to the associate production $gg,\, q\bar{q} \to tH^-\bar{b}$. Diagrams describing the quark-initiated parton processes are shown in Fig. 1, those describing the gluon-initiated processes, in Fig. 2. As explained in the introduction, if the center-of-mass energy of the relevant collider is sufficiently large to allow the tagging of two b-quarks in addition to the $H^\pm$-decay products, the measurement of the $2 \to 3$ production cross section may be possible.

The production cross section for a $p\bar{p}$ (pp) collider is obtained as usual by convoluting the hard scattering cross sections of the quark- and gluon-initiated processes with the quark- and gluon-distribution functions inside p and/or $\bar{p}$:

$$\sigma = \frac{1}{2s}\int_{\tau_{\rm min}}^1 \frac{d\tau}{\tau}\int_\tau^1 \frac{dx}{x}\int d{\rm PS}(q_1+q_2; p_1,p_2,p_3)\times \left\{\sum_q \Big[q(x,\mu_f)\bar{q}(\tau/x,\mu_f) + q \leftrightarrow \bar{q}\Big]|\mathcal{M}|^2_{q\bar{q}} + g(x,\mu_f)g(\tau/x,\mu_f)|\mathcal{M}|^2_{gg}\right\}, \qquad (2)$$

where q_i (p_i) are the four-momenta of the initial partons (final state particles), the functions $q(x,\mu_f)$, $\bar{q}(x,\mu_f)$ and $g(x,\mu_f)$ designate respectively the quark-, antiquark- and gluon-density functions with momentum fraction x at the factorization scale μ_f, and the index q in the sum, runs over the five flavors u, d, c, s, b. Finally, s is the hadron center-of-mass energy squared, whereas the parton center-of-mass energy squared is indicated, as usual, by $\hat{s} = x_1 x_2\, s \equiv \tau s$, with $\tau_{\rm min} = (m_{H^\pm}+m_t+m_b)^2/s$. The integration over $d{\rm PS}(q_1+q_2; p_1, p_2, p_3)$, an element of phase space of the 3–body final state, can be reduced to four nested integrals with bounds explicitly given in appendix A.

When rewriting the third generation vertex t-b-$H^\pm$ in (1) as $i(g/\sqrt{2})\,V_{tb}\,(v + a\,\gamma_5) + {\rm h.c.}$ with vector and axial couplings v and a given by:

$$v = \frac{1}{2}\left(\frac{m_b}{M_W}\tan\beta + \frac{m_t}{M_W}\cot\beta\right) ; \qquad a = \frac{1}{2}\left(\frac{m_b}{M_W}\tan\beta - \frac{m_t}{M_W}\cot\beta\right) , \tag{3}$$

the square amplitudes $|\mathcal{M}|^2_{gg}$ and $|\mathcal{M}|^2_{q\bar{q}}$ can be decomposed as:

$$\begin{aligned} |\mathcal{M}|^2_{q\bar{q}} &= (4\frac{G_F}{\sqrt{2}}M_W^2)\,(4\pi\alpha_S)^2\,|V_{tb}|^2\left(v^2\,V^{q\bar{q}} + a^2\,A^{q\bar{q}}\right) \\ |\mathcal{M}|^2_{gg} &= (4\frac{G_F}{\sqrt{2}}M_W^2)\,(4\pi\alpha_S)^2\,|V_{tb}|^2\left(v^2\,V^{gg} + a^2\,A^{gg}\right) . \end{aligned} \tag{4}$$

In this notations color factors are included in the reduced squared amplitudes $V^{q\bar{q}}$, $A^{q\bar{q}}$ and V^{gg}, A^{gg}, while the strong coupling constant is explicitly factored out. The expressions for the reduced amplitudes are too lengthy to be given here[1].

In the kinematical region $m_t > m_{H^\pm} + m_b$ the above cross section could be well approximated by the much simpler resonant production cross section, as given by the on-shell $t\bar{t}$ production cross section times the branching fraction for the decay $\bar{t} \to H^-\bar{b}$.

B. The $2 \to 3$ process: numerical results

The production cross section $\sigma(p\bar{p} \to tH^-\bar{b}X)$ for the Tevatron is shown by the solid lines in Fig. 3 as a function of the charged-Higgs mass for three different values of $\tan\beta$, $\tan\beta = 2$, 10, and 50, and in Fig. 4 as a function of $\tan\beta$ for different values of $m_{H^+} = 100$, 140, and 200 GeV. Notice that these figures show the cross section for single production of H^- only and that identical results are obtained for the process $\sigma(p\bar{p} \to \bar{t}H^+bX)$. All calculations are done at the leading order in QCD. The leading-order parton distribution functions CTEQ4L [26] are used in all calculations and the renormalization (μ_R) and factorization (μ_f) scales are always fixed to the threshold value $m_t + m_{H^\pm}$. The variation of these scales results in general in changes in the cross section presented here: a variation in the interval between $(m_t + m_{H^\pm})/2$ and $2(m_t + m_{H^\pm})$, can produce deviations up to $\pm 30\%$ with respect to the values shown in the figures. Higher-order corrections, therefore, may be important, as was shown in the case of associate production of the neutral Higgs. Their inclusion is called upon, but it is left for future work. As a cross-check of our cross-section calculation and phase space integration procedure, we have reproduced, by taking the appropriate limit, the well-known $gg, q\bar{q} \to t\bar{t}h$ cross-section [6] for the neutral Higgs h production in association with t-quarks.

As expected, the production cross section is enhanced in the resonance region $m_{H^\pm} < m_t - m_b$, when $H^\pm$ is obtained as a decay product of one of two t-quarks produced on-shell (see first diagram in Fig. 1 and the first and third diagrams in Fig. 2). The resonant t-quark propagator is regularized by the width of the t-quark, calculated from the SM decay $t \to bW^+$:

---

[1]The fortran code for these amplitudes is available upon request.

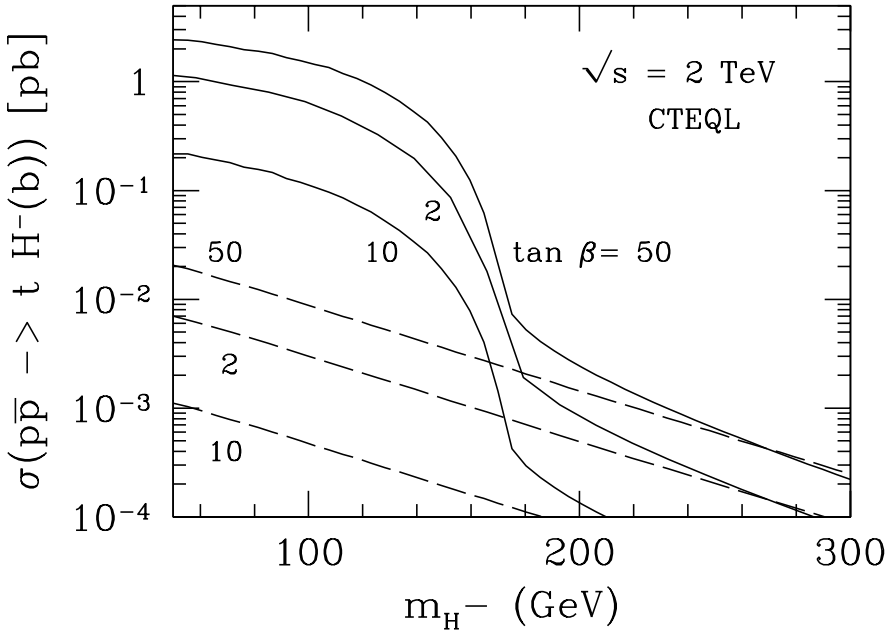

FIG. 3. The leading-order production cross section $\sigma(p\bar{p} \to t(\bar{b})H^- X)$ versus the charged Higgs mass, for $\sqrt{s} = 2\,\text{TeV}$ is shown for three different values of $\tan\beta = 2$, 10, 50. The solid lines indicate the cross sections obtained from $2 \to 3$ elementary processes $gg \to t\bar{b}H^-$ and $q\bar{q} \to t\bar{b}H^-$; the dashed lines show the cross sections obtained from the $2 \to 2$ process $gb \to tH^-$. Renormalization and factorization scales are fixed as $\mu_R = \mu_f = m_t + m_{H^-}$.

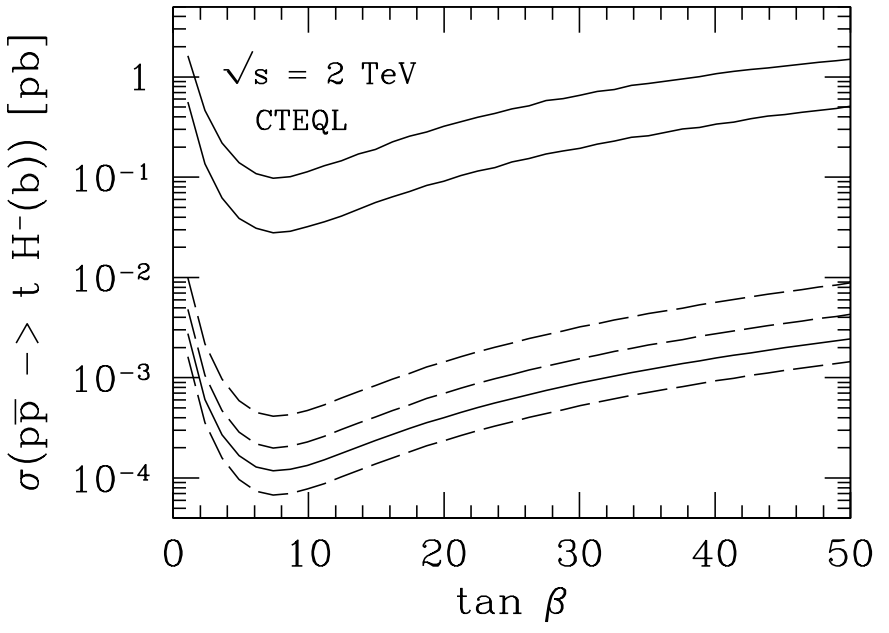

FIG. 4. The production cross section $\sigma(p\bar{p} \to t(\bar{b})H^-)$ is shown as a function of $\tan\beta$ for $m_{H^\pm} = 100$, 140, and 200 GeV (from top to bottom). As in Fig. 3, solid lines correspond to the $2 \to 3$ processes, dashed lines to the $2 \to 2$ process.

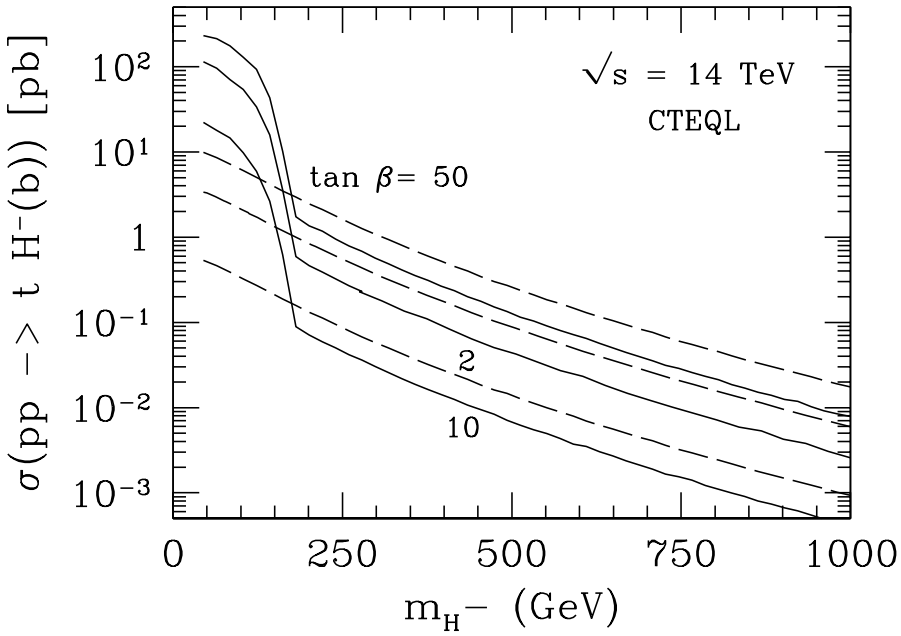

FIG. 5. The leading-order production cross section $\sigma(pp \to t(\bar{b})H^- X)$, for $\sqrt{s} = 14\,\text{TeV}$ is shown as a function of the charged Higgs mass for three different values of $\tan\beta = 2, 10, 50$. As in Figs. 3 and 4, the solid lines indicate the cross sections obtained from $2 \to 3$ elementary processes, the dashed lines, the cross sections obtained from the $2 \to 2$ process. Renormalization and factorization scales are fixed as $\mu_R = \mu_f = m_t + m_{H^-}$.

$$\Gamma(t \to bW^+) = \frac{g^2}{64\pi}|V_{tb}^*|^2 \frac{1}{m_t\, M_{W^+}^2}\left[M_{W^+}^2\left(m_t^2+m_b^2\right)+\left(m_t^2-m_b^2\right)^2-2M_{W^+}^4\right]\lambda^{1/2}\left(1,\frac{m_{W^+}^2}{m_t^2},\frac{m_b^2}{m_t^2}\right), \quad (5)$$

where λ is the Källen function $\lambda(x,y,z) = ((x^2-y^2-z^2)^2-4yz)$; and from the decay $t \to H^+ b$:

$$\Gamma(t \to H^+ b) = \frac{g^2}{32\pi}|V_{tb}^*|^2\, m_t \left\{v^2\left[\left(1+\frac{m_b}{m_t}\right)^2-\frac{m_{H^+}^2}{m_t^2}\right]+a^2\left[\left(1-\frac{m_b}{m_t}\right)^2-\frac{m_{H^+}^2}{m_t^2}\right]\right\}\lambda^{1/2}\left(1,\frac{m_{H^+}^2}{m_t^2},\frac{m_b^2}{m_t^2}\right), \quad (6)$$

for each value of $m_{H^\pm}$ and $\tan\beta$. In this region the cross section is not distinguishable from the convolution of $\sigma(p\bar{p} \to t\bar{t}X)$ with the branching fraction $Br(t \to H^+ b)$. The $\tan\beta$ dependence, shown explicitly in Fig. 4, has the same typical pattern of the branching ratio $Br(t \to H^+ b)$, i.e. large enhancements for very small and very large values of $\tan\beta$ and a minimum for $\tan\beta \simeq \sqrt{m_t/m_b}$. Away from the resonance region, the cross section diminishes rather rapidly and becomes negligible (at the Tevatron energy) for $m_{H^\pm} \gtrsim 250$ GeV.

Results qualitatively similar to those found for the Tevatron center-of-mass energy are obtained in the case of LHC searches. They are shown in Fig. 5. Assuming integrated

luminosity of 100 fb^{-1}, a significant production cross section is obtained for $m_{H^\pm} \lesssim 1\,\text{TeV}$ even for $\tan\beta = 10$, which is near the minimum of the production cross section.

Our results generalize those of Ref. [7], where contributions from the gluon-initiated diagrams were calculated for the LHC but only for $m_t = 150\,\text{GeV}$ and for a fixed $\tan\beta = 1$. Both of these values are now experimentally ruled out. We also note a disagreement between our calculation and that of Ref. [7], which could be, in part, due to our usage of a current set of structure functions. A similar calculation for the LHC case was also presented in Ref. [8], for different values of m_t. No immediate comparison with our results is, however, possible. The mechanism of associate production was also emphasized in Ref. [27] and a preliminary study was presented for the Tevatron center-of-mass energy [28].

C. The $2 \to 2$ process

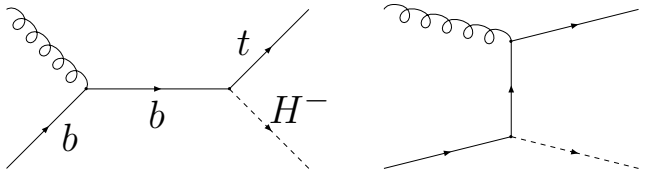

FIG. 6. Diagrams contributing to $p\bar{p}\,(pp) \to tH^- X$ through an elementary $2 \to 2$ process.

As mentioned in the introduction, for an inclusive measurement of single production of H^-, or if only one b-quark can be tagged besides the decay products of H^-, the elementary process $gb \to tH^-$ has to also be considered. The corresponding diagrams are shown in Fig. 6, and the hard scattering cross section reads:

$$\sigma(g\,b \to H^-\,t) = \left(4\frac{G_F}{\sqrt{2}}M_W^2\right)(4\pi\alpha_s)\,|V_{tb}|^2\frac{1}{192\pi\,\hat{s}\,(1-x_b^2)^3}\left\{8C_-x_bx_t\left[L\,(1-x_{ht}^2)-2\,b\right]+\right.$$

$$\left.C_+\left[2L\left(1+x_b^4-2x_b^2x_{ht}^2-2x_{ht}^2(1-x_{ht}^2)\right)-b\left(3-7x_{ht}^2+x_b^4(3+x_{ht}^2)+2x_b^2(1-x_{ht}^2)\right)\right]\right\}\,, \quad (7)$$

where $C_\pm = v^2 \pm a^2$; $x_i \equiv m_i/\sqrt{\hat{s}}$, $x_{ht}^2 = x_h^2 - x_t^2$; $b = [(1-(x_t+x_h)^2)(1-(x_t-x_h)^2)]^{1/2}$, and $L \equiv \ln\left[(1-x_{ht}^2+b)/(1-x_{ht}^2-b)\right]$.

The cross section originated from the $2 \to 2$ process only is shown in dashed lines in Figs. 3 and 4 for the upgraded Tevatron and in Fig. 5 for the LHC. (We note a disagreement with Ref. [12].) All calculations are again done at the leading-order in QCD, and renormalization and factorization scales are fixed as $\mu_R = \mu_f = m_{H^\pm} + m_t$. The cross sections are plagued by the same large uncertainties due to scale variations already observed in the case of the $2 \to 3$ processes. Notice that, away from the resonance region, $m_{H^\pm} < m_t - m_b$, the relative size of the two classes of cross sections depends on $\sqrt{s}$ and $m_{H^\pm}$. Indeed, at

high energies, where the gluon-initiated $2 \to 3$ processes dominate over the quark-initiated ones, the cross section arising from the elementary process $gb \to tH^-$ is larger than that from $2 \to 3$ ones, which is penalized by a 3-body phase space suppression. At the Tevatron center-of-mass energy, the quark-initiated $2 \to 3$ processes have still the dominant role for not too large values of $m_{H^\pm}$. For the particular choice of scales μ_R and μ_f made here, the cross-over for the two cross sections is at about $m_{H^\pm} \sim 265\,\mathrm{GeV}$.

D. The inclusive single $H^\pm$ production cross section

Before presenting the inclusive cross section, some elaboration on the summation procedure used to add the $2 \to 3$ and $2 \to 2$ channels is in order. Since the initial b-quark is contained in the proton or antiproton via a gluon, the $2 \to 2$ process is of the same order in α_s as the $2 \to 3$ ones. The collinearity of the b-quark with the initial gluon induces the large factor $\alpha_s(\mu_R)\log(\mu_f/m_b)$, where the factorization scale μ_f is $\mathcal{O}(m_{H^\pm})$ and it was chosen to be $\mu_f = m_t + m_{H^\pm}$ in our numerical evaluations. This factor is then resummed to all orders $(\alpha_s(\mu_R)\log(\mu_f/m_b))^n$ when making use of the phenomenological b-distribution function. The first order $n = 1$, is also contained in the set of $2 \to 3$ partonic processes $gg \to tH^-\bar{b}$ when one of the two initial gluons produces a pair $b\bar{b}$ collinear to the initial p ($\bar{p}$). (See the last two diagrams of Fig. 2.) Thus, when summing the contributions from $2 \to 2$ and $2 \to 3$ cross sections, this term has to be properly subtracted in order to avoid double counting. Given the relevance of resummation for the large parameter $\alpha_s(\mu_R)\log(\mu_f/m_b)$, it is often concluded that the $2 \to 2$ process gives the bulk of the cross-sections for the single production of $H^\pm$. As it was already noticed in the previous sections, however, the issue of dominance of one cross section over the other, depends on $\sqrt{s}$ and $m_{H^\pm}$.

The summation and subtraction procedure has been carefully systematized in the case of production of neutral Higgs bosons [29,10], for which, in a similar way, also the $2 \to 1$ process, $\bar{b}b \to H^0$, and $2 \to 2$ one, $gb \to bH^0$, partially overlap. It was applied to the case of charged Higgs production in Ref. [30], where it was debated whether a $2 \to 1$ elementary process $t\bar{b} \to H^+$ also contributes to the inclusive cross section, once the theoretically calculated t-distribution function is folded in the proton beam. For the ranges of $m_{H^\pm}$ that may be probed at the Tevatron and at the LHC, the term $\log(m_H/m_t)$ is sufficiently small, and the $2 \to 1$ process can be safely omitted [30]. We therefore disregard the process $t\bar{b} \to H^+$ in our analysis and in addition assume sufficient b-tagging efficiency so that final states with three or more b's can be distinguished [8,31].

Following Refs. [29,10], we introduce the distribution function $\tilde{b}(x,\mu_f)$ given by the perturbative solution to the Dokshitzer–Gribov–Lipatov–Altarelli–Parisi equation:

$$\tilde{b}(x,\mu_f) = \frac{\alpha_s(\mu_R)}{\pi}\ln(\frac{\mu_f}{m_b})\int_x^1 \frac{dy}{y} P_{gb}\left(\frac{x}{y}\right) g(y,\mu_f) \tag{8}$$

where the splitting function is $P_{gb}(x) = (x^2 + (1-x)^2)/2$ and $g(x,\mu_f)$ is the usual gluon-distribution function at the factorization scale μ_f. The hard process $gb \to tH^-$, convoluted with the distribution function $\tilde{b}$ above, gives a contribution which has to be subtracted

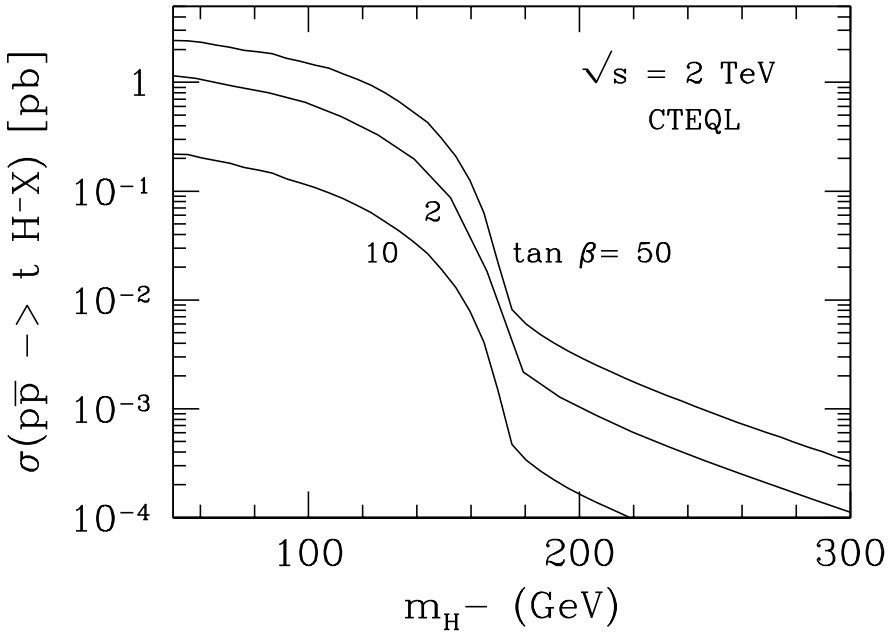

FIG. 7. The leading-order production cross section $\sigma(p\bar{p} \to tH^- X)$, for $\sqrt{s} = 2\,\text{TeV}$, as a function of the charged Higgs mass, is shown for three different values of $\tan\beta = 2$, 10, 50. The cross section is obtained by adding the contribution of the $2 \to 2$ process, $gb \to tH^-$, to those of the $2 \to 3$ ones, $gg \to t\bar{b}H^-$ and $q\bar{q} \to t\bar{b}H^-$, and subtracting overlapping terms. Renormalization and factorization scales are fixed as $\mu_R = \mu_f = m_t + m_{H^-}$.

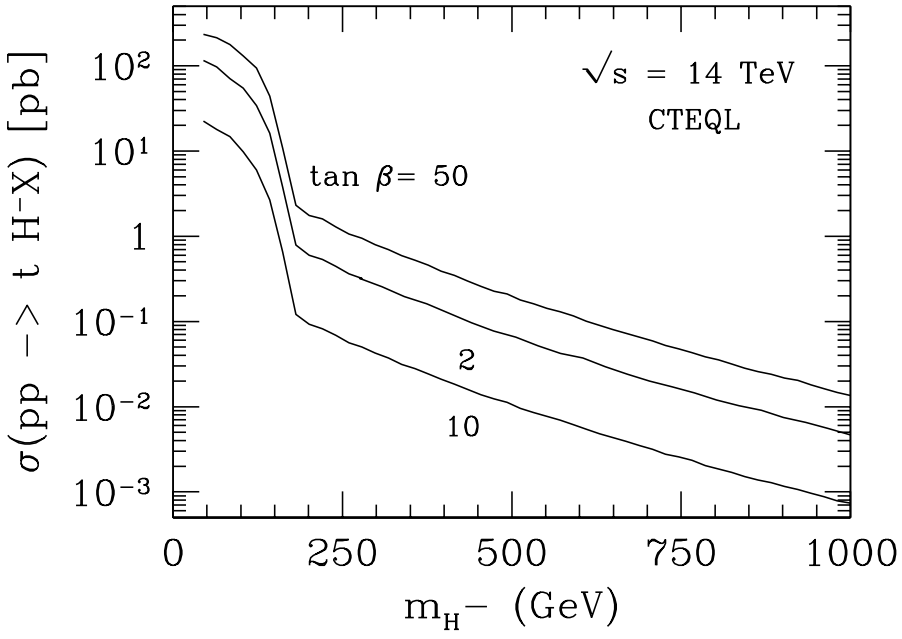

FIG. 8. Same as in Fig. 7 for center-of-mass energy $\sqrt{s} = 14\,\text{TeV}$.

from the sum of the gg-initiated and (standard) gb-initiated process, convoluted with the phenomenological b-distribution function.

The appropriately summed inclusive cross section is shown in Fig. 7 for the Tevatron and in Fig. 8 for the LHC. As in the case of only the $2 \to 3$ channels, a potential reach of ~ 250 GeV and of $\mathcal{O}(1)$ TeV is found, respectively, for the Tevatron (with 10–30 fb^{-1} luminosity) and the LHC (with a luminosity of 100 fb^{-1} per year). Background and other detection and identification considerations will somewhat diminish this reach [8], which is therefore given only as a rough guideline.

III. SLEPTON–STRAHLUNG

In supersymmetric models, lepton L and baryon B numbers are not accidental symmetries, but have to be imposed by hand, e.g., by imposing a discrete R–symmetry (R–parity) [32] $R_P = (-1)^{B+3L+J}$ where J is the particle spin. It is possible, however, that only L or B correspond to a conserved number, which is sufficient to ensure the proton stability. In particular, in supersymmetry the lepton and Higgs doublets are not distinguished by their spin as in the SM. It is therefore natural to expect that some mixing exists between slepton and Higgs bosons as well as leptons and higgsinos that carry the same quantum numbers, and, hence, that lepton number L is generically not conserved. The realization of L-violation is basis dependent and it is usually convenient to define the two Higgs doublets as those whose neutral components are aligned along the two large vevs; the lepton doublets along the orthogonal directions in field space. In this basis it is straightforward to show that neutrino masses arise from small tree-level mixing with the neutralinos and at one- and two-loop levels from $\Delta L = 1$, Yukawa-type interactions [33–36]. This offers an exciting avenue for generating neutrino mass and mixing at the weak scale. It further suggests collider tests of models of neutrino masses since both radiative neutrino masses and slepton production are controlled by the same Yukawa couplings.

In the following, only models in which lepton number is violated by $\Delta L = 1$ renormalizable operators are considered. The low-energy lagrangian is derived from the superpotential operator

$$W = \lambda'_{lmn} L_l Q_m D_n \,, \tag{9}$$

where L, Q, D are the lepton and quark doublet and down singlet superfields, respectively. The possibility of renormalizable purely leptonic operators, also involving a $\Delta L = 1$ lepton-number violation, do not affect our analysis and are neglected hereafter. In component fields, the slepton-quark interactions relevant for our purposes are:

$$\mathcal{L}_{\not L} \;\supset\; \lambda'_{lmn} V_{mj}\, \overline{u}_{Lj}\, d_{Rn} \tilde{e}^*_{Ll} \;-\; \lambda'^*_{lmn}\, \overline{d}_{Lm}\, d_{Rn} \tilde{\nu}^*_{Ll} + \text{h.c.}\,, \tag{10}$$

where $\tilde{f}$ denotes the sfermion superpartner of a fermion f and all generation indices are arbitrary. In deriving (10) it was assumed that the right-handed quark fields as well as the left-handed down-quark fields are already in the mass eigenstate basis and the CKM matrix

V coincides with the rotation matrix of the left-handed up-quark sector. Had this assumption not been made, both fermions in each of the two terms of eq. (10) would be multiplied by the appropriate rotation matrix. However, in the absence of any initial assumption on the texture of the λ' matrix, this would merely correspond to a redefinition of its elements.

The $\Delta L = 1$ couplings given above cannot be arbitrarily large as they lead to tree-level corrections to various observables and correct neutral and charged current universality [37]. With the exception of $\lambda'_{111} \lesssim 10^{-4}$ and $\lambda'_{1m1} \lesssim 10^{-2}$ from $(\beta\beta)_{0\nu}$-decay and atomic parity violation, respectively, one has $\lambda'_{11n} \lesssim 0.01$, $\lambda'_{l2n} \lesssim 0.2$, and $\lambda'_{l3n} \lesssim 0.4 - 0.5$, for sfermions with masses of 100 GeV. These constraints and their derivation are summarized, for instance, in Ref. [38]. As an example, the weak constraints on λ'_{l3n} are derived from either t-quark decays [39,40] (this constraint, however, vanishes as the slepton mass approaches the t-quark mass), from the one standard deviation in the Z width [41], or from b-quark semileptonic decays [40,42], again at one standard deviation. The above constraints scale as a power of $m_{\tilde{f}}$ and are therefore significantly weaker for heavier sfermions. For example, for squarks near the 500 GeV mark, $\lambda' \sim 1$ in the third family is generally not excluded. On the other hand, constraints on pairs of non-identical couplings (e.g., from meson mixing) often imply further that certain combination of couplings cannot saturate their individual upper bounds simultaneously. In general, the hierarchy of couplings that emerges from experiment is similar to the generational hierarchy in the usual Yukawa couplings (with λ'_{333} the most weakly constrained), an observation that we will adopt as a guideline. (A similar structure is also suggested by various theoretical models. See, for example, Ref. [33,35].)

A. Production cross section

The terms (10) in the Lagrangian lead to new and exciting possibilities for slepton production at hadron colliders: (*i*) exotic t-quark decays $t \to \tilde{\tau} b$, if kinematically allowed [39,40,43], (*ii*) s-channel resonant production of sleptons [44] (see, e.g., Ref. [40] for a discussion of resonant production at LEP), and, as proposed above, (*iii*) associate production $qq'\tilde{l}$. (In addition, (*iv*) gluonic couplings are induced for the sneutrino which could now be singly produced $gg \to \tilde{\nu}$ [45].) Here, we focus on the charged-slepton–strahlung production, in particular, stau $\tilde{\tau}$ production in association with t and b-quarks. Associate production of the neutral sleptons will be discussed elsewhere [45]. Both $2 \to 2$ and $2 \to 3$ channels $gb \to t\tilde{\tau}^-$ and gg, $qq \to t\tilde{\tau}^-\bar{b}$, will be considered (at the leading order) and properly combined. As in the case of the charged Higgs production, the $2 \to 3$ processes encompass the production mechanism (*i*) in the relevant kinematic region.

For concreteness, the only R–parity violating coupling which is considered is λ'_{333}. This choice is motivated by the fact that this is the least constrained coupling, and, as explained above, it is expected to be the most significant among the $\Delta L = 1$ couplings in some frameworks. In this case, the cross-section scales as λ'^2_{333} in the kinematic region $m_t < m_{\tilde{\tau}} + m_b$. In the complementary region $m_t \gtrsim m_{\tilde{\tau}} + m_b$, sleptons contribute to the width of the t-quark (in proportion to λ'^2_{333}) violating this simple scaling law. This implies that though our results may be taken as indicative for cases involving other λ' couplings, they cannot be used directly in cases not involving the t-quark. In addition, the subtraction procedure

to be followed when combining the different $2 \to 2$ and $2 \to 3$ channels into the inclusive cross section, although conceptually similar, differs technically for cases with one or two light quarks associated to the $\tilde{\tau}$-production. For this reason also, the results presented here cannot be simply adapted to production cross sections involving other λ' couplings or to the case of neutral-slepton production. (The latter is also complicated by the presence of the gluon fusion channel.) On the other hand, the slepton generation label does not enter our calculation but affects only the signal analysis (on which we comment below). Hence, our results can be generalized in a straightforward fashion to the production of other charged sleptons in association with t- and b-quarks.

It should be noted that the produced slepton is always left-handed, as a result of the structure of the operator (10). Of course, the physical eigenstates are, in general, admixtures of left- and right-handed current eigenstates. For simplicity, it is assumed in the following that the left–right mixing term in the $\tilde{\tau}$ mass squared matrix is small. As a consequence, left- and right-handed current eigenstates coincide already with the two mass eigenstates, with mass $m_{\tilde{\tau}_L}$ and $m_{\tilde{\tau}_R}$. The first of these two masses recurrent in this analysis will be simply denoted as $m_{\tilde{\tau}}$. (A generalization is straightforward and involves the introduction of a mixing angle.)

The inclusive production cross sections $p\bar{p} \to t\tilde{\tau}_L X$, $pp \to t\tilde{\tau}_L X$ are obtained by combining the production cross sections arising from the $2 \to 2$ elementary process $gb \to t\tilde{\tau}_L$ to those induced by $2 \to 3$ partonic processes, which give rise to $p\bar{p} \to t\bar{b}\tilde{\tau}_L X$, $pp \to t\bar{b}\tilde{\tau}_L X$. The $2 \to 3$ processes might be independently measured only if relatively complicated final states could be detected. The corresponding inclusive cross sections, formally given by eq. (2), is obtained by convoluting the hard scattering cross section of quark- and gluon-initiated processes with the quark and gluon distribution functions in p ($\bar{p}$). The Feynman diagrams for the partonic processes are those of Figs. 1 and 2 with H^- replaced by $\tilde{\tau}_L$. Since the vector and axial coupling v and a for the vertex t-b-$\tilde{\tau}_L$ are now simply $v = a = 1/2$, the square amplitudes $|\mathcal{M}|^2_{gg}$ and $|\mathcal{M}|^2_{q\bar{q}}$ can be decomposed as:

$$\begin{aligned} |\mathcal{M}|^2_{q\bar{q}} &= \frac{1}{4}\lambda'^2_{333}\,(4\pi\alpha_S)^2\,|V_{tb}|^2\,(V^{q\bar{q}} + A^{q\bar{q}}) \\ |\mathcal{M}|^2_{gg} &= \frac{1}{4}\lambda'^2_{333}\,(4\pi\alpha_S)^2\,|V_{tb}|^2\,(V^{gg} + A^{gg})\ . \end{aligned} \tag{11}$$

The reduced square amplitudes $V^{q\bar{q}}$, $A^{q\bar{q}}$ and V^{gg}, A^{gg} coincide with those obtained for the $2 \to 3$ charged Higgs production processes, once the replacement $m_{H^\pm} \to m_{\tilde{\tau}_L}$ is made. In the kinematical region of a resonant t-quark, only the two decay modes $t \to W^+ b$ and $t \to \tilde{\tau}^+ b$, which has the width

$$\Gamma(t \to \tilde{\tau}^+ b) = \frac{\lambda'^2_{333}}{32\pi}\, m_t |V^*_{tb}|^2 \left(1 + \frac{m_b^2}{m_t^2} - \frac{m_{\tilde{\tau}}^2}{m_t^2}\right) \lambda^{1/2}\left(1, \frac{m_{\tilde{\tau}}^2}{m_t^2}, \frac{m_b^2}{m_t^2}\right)\ , \tag{12}$$

are considered. For simplicity, the charged Higgs $H^\pm$ is assumed to be sufficiently heavy, as to kinematically forbid the decay mode $t \to H^+ b$.

If only the t-quark can be detected in addition to the decay products of $\tilde{\tau}_L$, the contribution from the $2 \to 2$ process has to be included. The Feynman diagrams for this process

are those of Fig. 6 with the obvious substitution $H^- \to \tilde{\tau}_L$; the hard scattering cross section is obtained from (7) by replacing $4G_F M_W^2/\sqrt{2}$ with $\lambda'_{333}/2$ and m_{H^-} with $m_{\tilde{\tau}_L}$. The subtraction procedure to avoid double counting follows exactly the pattern already described for the production of the charged Higgs boson. The final inclusive production cross sections $\sigma(p\bar{p}, pp \to t\tilde{\tau}X)$ are shown in Figs. 9 and 10 for the Tevatron and the LHC, respectively as function of the $\tilde{\tau}_L$ mass $m_{\tilde{\tau}_L} \gtrsim 45$ GeV. Note that, since lepton-number is violated, we conservatively apply the model-independent lower limit $m_{\tilde{\tau}} \gtrsim 45$ GeV extracted from the measurement of the Z width.

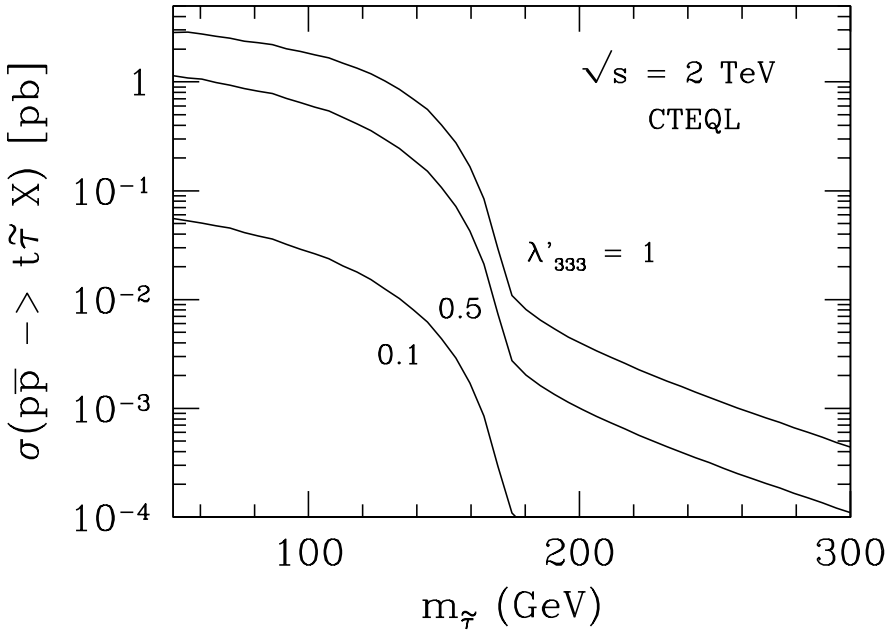

FIG. 9. The leading-order production cross section $\sigma(p\bar{p} \to t\tilde{\tau}X)$, for $\sqrt{s} = 2\,\text{TeV}$, as a function of the $\tilde{\tau}$ mass is shown for different values of λ'_{333}. Renormalization and factorization scales are fixed as $\mu_R = \mu_f = m_t + m_{\tilde{\tau}}$.

The large cross section obtained in the case of $\sqrt{s} = 14\,\text{TeV}$ implies that at the LHC, with luminosity of 100 fb^{-1} per year, light $\tilde{\tau}$'s may be produced in abundance even for couplings as small as 0.01, whereas for large couplings, they may be produced up to masses of $\mathcal{O}(1)\,\text{TeV}$.

The $\tilde{\tau}$-decay modes are highly model dependent in the case of lepton-number violation. In particular, all superpartners typically decay in the collider and the typical large missing energy signature is replaced with multi-b, and lepton signatures which may be used for identification. (See, for example, Ref. [46].) Depending on couplings and phase space, the main two-body decays for $\tilde{\tau}$ are, for example: $\tilde{\tau} \to \tilde{\chi}^0\tau$, $\tilde{\chi}^\pm\nu_\tau$, tb, cb, ts, $l\nu$, where we included the effect of purely leptonic couplings. (There exist also two-body decays due to tree-level Higgs-slepton, chargino-tau, and neutralino-neutrino mixing. These are, however, strongly suppressed by the small mixing angle $\sim (m_\nu/m_Z)^2$.) In addition, various three-body decay channels may be open, depending on the model parameters. The charginos and neutralinos, if produced, also cascade in a model-dependent way to leptons and jets. Therefore, detec-

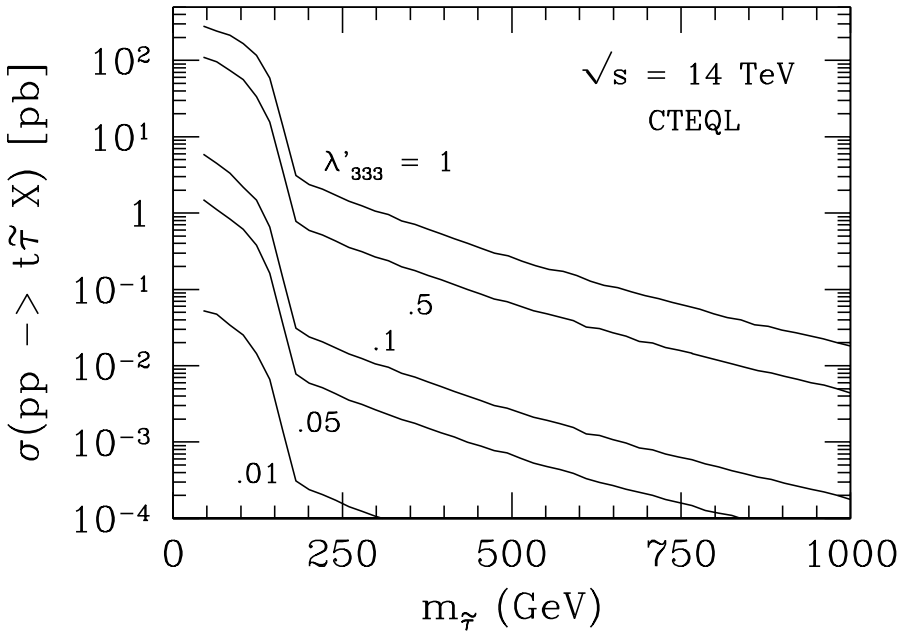

FIG. 10. The leading-order production cross section $\sigma(pp \to t\tilde{\tau}X)$, for $\sqrt{s} = 14\,\text{TeV}$, as a function of the $\tilde{\tau}$ mass is shown for different values of λ'_{333}. Renormalization and factorization scales are fixed as $\mu_R = \mu_f = m_t + m_{\tilde{\tau}}$.

tion and background studies cannot be done in a model- (coupling-) independent fashion. Particularly so, once our assumption that only the charged Higgs or the stau (but not both) are produced in association with t is generalized. Nevertheless, many promising multi-lepton and multi-b signatures are available. The study of detection aspects is well motivated by the potential reach in small coupling and/or large mass, but it is left for future works.

Leaving detection issues aside, in L-violating models, sleptons are potentially more accessible (depending on the coupling) than in models with lepton-number conservation where their direct production relies on the Drell-Yan process which allows discovery reach for sleptons only up to $m_{\tilde{l}} \lesssim 350$ GeV at the LHC [47]. (Cascade decays may provide the bulk of slepton production in the lepton number conserving models but such processes are highly model dependent. They also complement slepton production in the lepton number violating case studied here.) The potential reach at the Tevatron is limited to large couplings and/or light $\tilde{\tau}$'s. Nevertheless, the slepton–strahlung provides a unique slepton-discovery mechanism at the Tevatron as well.

B. Exploring $\Delta L = 1$ models of neutrino masses

An obvious question is to what extent does the discovery reach described above enable one to explore the corresponding models of neutrino masses. It is straightforward to show that the supersymmetry-rotated operators (10) with a quark (sneutrino) replaced by a squark

(neutrino) lead, at one-loop order, to a Majorana neutrino mass as illustrated in Fig. 11. One obtains

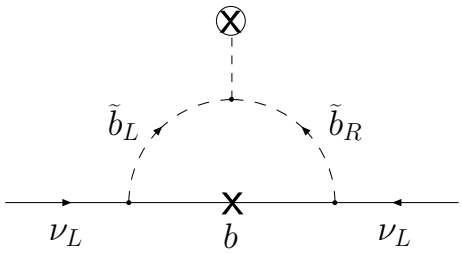

FIG. 11. An one-loop contribution to the Majorana neutrino mass arising from the $\Delta L = 1$ operators of the superpotential (9).

$$\frac{m_\nu}{\mathrm{M}eV} \sim \lambda'^2 \left(\frac{300\,\mathrm{G}eV}{m_{\tilde{b}}}\right)\left(\frac{m^2_{LR}}{m_b\, m_{\tilde{b}}}\right) , \tag{13}$$

where a b-quark and $\tilde{b}$-squark are assumed to circulate in the loop and m^2_{LR} is the $\tilde{b}$ left-right mixing squared mass. (Note that the size m^2_{LR} here can be significant even if left-right stau mixing is suppressed.) The neutrino mass may vanish in the limit of a continuous $\mathrm{U}(1)_R$ symmetry which corresponds in our case to $m^2_{LR} \ll m_b\, m_{\tilde{b}}$. It is further assumed that no other accidental cancellation among various contributions to the neutrino mass take place. In this case, the contribution (13), if exists, constitutes probably the dominant contribution to the neutrino mass (Another contribution may arise from tree-level neutrino-neutralino mixing.) Imposing laboratory limits on the ν_e mass one can, for example, derive severe constraints on λ'_{133} [48].

Given all other constraints and the cross sections of Figs. 9 and 10, λ'_{233} and λ'_{333} are the couplings which are likely to be probed at hadron colliders through slepton–strahlung production. Assuming that associate stau production can be observed for $\lambda' \gtrsim 0.1\,(0.01)$ one can explore neutrino masses heavier than 3 KeV (30 eV), for $m_{\tilde{b}} \lesssim 1\,\mathrm{TeV}$ and $m_b\, m_{\tilde{b}}/m^2_{LR}$ of $\mathcal{O}(1)$ in (13). It is interesting to note that if the coupling is large enough to lead to slepton production, the corresponding neutrino cannot probably be in sub-eV range, as is sometimes assumed, unless the $\tilde{b}$-squarks are in the multi-TeV range, and with negligible left-right mixing. Furthermore, a large slepton production cross section, may even imply a heavy neutrino species which decays on cosmological time scales. Alternatively, if the $\tilde{b}$-squarks are not discovered at the LHC (when considering the R_P violating cascades), the same range of coupling would automatically imply much lighter neutrinos, possibly in the sub-eV range, enhancing the coverage of the neutrino-mass parameter space.

Thus, collider studies in this case carry indirect but crucial implications to models of neutrino masses and can help reveal the neutrino spectrum. This beneficial relation is due to supersymmetry which relates the neutrino radiative mass operators and the slepton-quark Yukawa operators. Negative search results can alternatively provide strong constraints on the λ'_{i33} couplings, especially if slepton masses are independently measured. Such potentially strong constraints are currently not available by any other method. Further handles on the

couplings and on the neutrino spectrum are provided by the search for the sneutrinos [45], in which case also the gluon fusion $gg \to \tilde{\nu}$ channel is available. The gluon-fusion cross section also depends quadratically on λ' Yukawa couplings, and it is given by a straightforward generalization of the Higgs gluon-fusion $gg \to H^0$ cross section [45].

IV. SUMMARY AND OUTLOOK

In summary, we have shown that charged Higgs– and slepton–strahlung provide important channels of single production. Our study implies a significant production cross section, in particular at LHC, but also at the upgraded Tevatron energies. For example, charged Higgs bosons and staus as heavy as one TeV can be produced at the LHC (Figs. 5 and 10). For lighter staus, R–parity violating couplings as small as 0.01 may be probed (Fig. 10). At the Tevatron (Figs. 7 and 9), the kinematic reach may be significantly extended in comparison to that obtained from the t-quark decays $t \to H^+ b$ and $t \to \tilde{\tau}^+ b$ Of course, more conclusive statements should await detailed background and detection studies.

Our calculations, at the leading order, include exact evaluation of the three-body phase space and special attention was given to the correct summation of the various contributions to the inclusive cross section.

The importance of b-tagging in separating the various channels was pointed out. In addition, various weakly interacting particles may be produced simultaneously in association with quarks (*e.g.*, the charged Higgs and one or two charged sleptons), hence, raising the issue of their separation and identification. In particular, in the case of the stau studied here, the slepton signature could be similar to that of the charged Higgs. (Similarly, the neutral Higgs and sneutrino could be both produced via gluon fusion and/or strahlung and could also decay similarly, extending the problem to the neutral sector as well.) One may have to rely on mass differences and on more suppressed L-violating or supersymmetric decays in order to distinguish the different bosons.

Detection of singly produced sleptons via the strahlung process (or any other process) carries substantial benefits to the mapping of the lepton number violating potential (and superpotential). Hence, it also carries important consequences to models in which neutrino masses are obtained radiatively, since radiative neutrino masses are proportional to the couplings of the slepton-quark Yukawa operators. Leaving detection issues aside, heavy sleptons could be abundantly produced in L-violating models and small L-violating couplings (and hence, small neutrino masses) may be probed.

Though not discussed explicitly, a similar situation to that studied in this paper can arise in any other model in which a weakly interacting scalar couples via a non-negligible Yukawa coupling to quarks. The most obvious example, which corresponds to a straightforward generalization of the slepton–strahlung case, is given by (scalar) lepto-quark models.

ACKNOWLEDGMENTS

It is pleasure to thank H. Frisch and G. Moultaka for discussions. This work was supported by CNRS and by the US Department of Energy under contract No. DE-FG02-96ER40559. NP wishes to thank the theory group at CERN for its hospitality.

APPENDIX A: THREE BODY PHASE SPACE

In eq. (2) $d\mathrm{PS}\,(q_1+q_2;p_1,p_2,p_3)$ is an element of the 3–body final state phase space normalized as [17]

$$\begin{aligned}\int d\mathrm{PS} &= \int (2\pi)^4\,\delta^4(q_1+q_2-p_1-p_2-p_3)\,\frac{d^3p_1}{(2\pi)^3 2E_1}\,\frac{d^3p_2}{(2\pi)^3 2E_2}\,\frac{d^3p_3}{(2\pi)^3 2E_3}\,;\\ &\to \frac{1}{(2\pi)^4}\frac{1}{8}\int_{-1}^{+1} d(\cos\theta)\int_0^{2\pi} d\phi\int_{E_1,\min}^{E_1,\max} dE_1\int_{E_{12},\min}^{E_{12},\max} dE_{12}\,, \end{aligned} \tag{A1}$$

where q_i (p_i) are the four-momenta of the initial partons (final state particles) and E_1, E_2 can be chosen e.g. as the energies of the final t and b respectively, with $E_{12}\equiv(E_1-E_2)/2$, and E_3 the energy of the $H^\pm$. The remaining integral in eq. (A1) is over appropriately defined angles θ and ϕ, describing the motion with respect to the beam axis of the 3–momenta $\mathbf{p}_1$, $\mathbf{p}_2$ of the two produced quarks. (Of the initial four angular integrations, one is eliminated from energy conservation and another (azimuthal) angle integration simply gives a factor of 2π included in eq. (A1).) The integration bounds for the energy E_1 are as follows:

$$E_{1,min}=m_t\,;\qquad E_{1,max}=\frac{\hat{s}+m_t^2-\left(m_b+m_{H^\pm}\right)^2}{2\sqrt{\hat{s}}}\,; \tag{A2}$$

those for the energy E_2:

$$E_{12,min/max}=\frac{-b\mp\sqrt{b^2-4ac}}{2a}\,, \tag{A3}$$

with a, b, and c given by:

$$\begin{aligned} a &= 2E_1\sqrt{\hat{s}}-\hat{s}-m_t^2\\ b &= -\left(\sqrt{\hat{s}}-E_1\right)\left(m_{H^\pm}^2-m_b^2\right)\\ c &= \frac{1}{4}\left\{\left(E_1^2-m_t^2\right)\left[\left(\sqrt{\hat{s}}-E_1\right)^2-4m_b^2\right]-\left(E_1^2+m_{H^\pm}^2-m_t^2-m_b^2\right)^2\right\}. \end{aligned} \tag{A4}$$

Finally, the resulting six-dimensional integral eq. (2) over the remaining phase space and over the parton luminosities is performed numerically with the standard Vegas Monte-Carlo integration routine [49].

REFERENCES

[1] F. Wilczek, Phys. Rev. Lett. **39** (1977) 1304;
H. Georgi, S.L. Glashow, M.E. Machacek, and D.V. Nanopoulos, Phys. Rev. Lett. **40** (1978) 692;
S. Dawson, Nucl. Phys. B359 (1991) 283;
A. Djouadi, M. Spira, and P. Zerwas, Phys. Lett. **B264** (1991) 440;
M. Spira, A. Djouadi, D. Graudenz, and P.M. Zerwas, Nucl. Phys. B453 (1995) 17;
S. Dawson, A. Djouadi, and M. Spira, Phys. Rev. Lett. 77 (1996) 16.

[2] F.M Borzumati and A. Djouadi, hep-ph/9806301.

[3] F.M. Borzumati and N. Polonsky, in e^+e^- *Collisions at TeV Energies*, P. Zerwas (Ed.), DESY-96-123D, p.41, hep-ph/9602433;
E. Accomando *et al.*, Phys. Rep. **299** (1998) 1.

[4] J.A. Coarasa, J. Guasch, J. Sola, and W. Hollik, hep-ph/9808278;
J.A. Coarasa, D. Garcia, J. Guasch, R.A. Jiménez, and J. Solà, Eur. Phys. J. **C2** (1998) 373;
J. Guasch and J. Solà, Phys. Lett. **B416** (1998) 353.

[5] for a list of older references see, for example, F. Borzumati, in e^+e^- *Collisions at 500 GeV*, P. Zerwas (Ed.), DESY 93-099, p. 261-268, hep-ph/9310348.

[6] Z. Kunszt, Nucl. Phys. **B247** (1984) 339;
J. Dai, J.F. Gunion, and R. Vega, Phys. Rev. Lett 71 (1993) 2699;
Z. Kunszt, S. Moretti, and W. J. Stirling, Z. Phys. **C74** (1997) 479;
M. Spira, Fortsch. Phys. **46** (1998) 203, hep-ph/9705337.

[7] J.L. Diaz-Cruz and O.A. Sampayo, Phys. Rev. **D50** (1994) 6820.

[8] J.F. Gunion, Phys. Lett. **B322** (1994) 125.

[9] D. Dicus and S. Willenbrock, Phys. Rev. **D39** (1989) 751.

[10] D. Dicus, T.Stelzer, Z. Sullivan, and S. Willenbrock, hep-ph/9811492.

[11] A.C. Bawa, C.S. Kim, and A.D. Martin, Z. Phys. **C47** (1990) 75;
S. Moretti and K. Odagiri, Phys. Rev. **D55** (1997) 5627.

[12] C.S. Huang and S.H. Zhu, hep-ph/9812201.

[13] A. Djouadi, S. Rosier-Lees *et al.*, *Report of the MSSM Working Group for the GDR–Supersymètrie*, hep–ph/9901246.

[14] A. Stange, W. Marciano, and S. Willenbrock, Phys. Rev. **D49** (1994) 1354;
M.C. Smith and S.S. Willenbrock, Phys. Rev. **D54** (1996) 6696.

[15] D.A. Dicus, J.L. Hewett, C. Kao, and T.G. Rizzo, Phys. Rev. **D40** (1989) 787;
A.A. Barrientos Bendezu and B.A. Kniehl, hep-ph/9807480;
S. Moretti and K. Odagiri, hep-ph/9809244.

[16] A. Djouadi, J.-L. Kneur, and G. Moultaka, Phys. Rev. Lett. **80** (1998) 1830.

[17] A. Djouadi, J-L. Kneur and G. Moultaka, hep-ph/9903218.

[18] A. Dedes and S. Moretti, hep-ph/9812328;
A. Dedes and S. Moretti, hep-ph/9904491.

[19] A. Krause, T. Plehn, M. Spira, and P.M. Zerwas, Nucl. Phys. **B519** (1998) 85.

[20] F. Borzumati and N. Polonsky, in preparation.

[21] A. Belyaev, M. Drees, O.J.P. Eboli, J.K. Mizukoshi, and S.F. Novaes, hep-ph/9905266

[22] F. Borzumati and C. Greub, Phys. Rev. **D58** (1998) 074004; *ibid.* **D59** (1999) 057501; and hep-ph/9810240.
[23] Review of Particle Physics, C. Caso et al., Eur. Phys. J. C **3** (1998) 1.
[24] For a general review, see M. Spira in Ref. [6];
M. Spira and P.M. Zerwas, hep-ph/9803257;
M. Spira, hep-ph/9810289.
[25] See, for example, M. Carena, S. Mrenna, and C.E.M. Wagner, hep-ph/9808312.
[26] CTEQ Collaboration, H.L. Lai *et al.*, Phys. Rev **D55** (1997) 1280.
[27] J.A. Coarasa, D. Garcia, J. Guasch, R.A. Jimenez, and J. Sola, Phys. Lett. **B425** (1998) 329.
[28] J. Sola, talk presented at the Higgs and Supersymmetry RUN II Workshop, Fermilab, Batavia, IL, November 1998.
[29] R.M. Barnett, H.E. Haber, and D.E. Soper, Nucl. Phys. **B306** (1988) 697;
R.M. Barnett, H.E. Haber, F.E. Paige, and D.E. Soper, Nucl. Phys. **B306** (1988) 697;
F.I. Olness and W.-K. Tung, Nucl. Phys. **B308** (1988) 813;
D. Dicus and S. Willenbrock, Phys. Rev. **D39** (1989) 751.
[30] J.F. Gunion, H.E. Haber, F.E. Paige, W.K. Tung, and S.S.D. Willenbrock, Nucl. Phys. **B294** (1987) 621.
[31] V. Barger, R.J.N. Phillips, and D.P. Roy Phys. Lett. **B324** (1994) 236.
[32] G. Farrar and P. Fayet, Phys. Lett. **B76** (1978) 575.
[33] L.J. Hall and M. Suzuki, Nucl. Phys. **B231** (1984) 419.
[34] T. Banks, Y. Grossman, E. Nardi, and Y. Nir, Phys. Rev. **D52** (1995) 5319;
F.M. Borzumati, Y. Grossman, E. Nardi, and Y. Nir, Phys. Lett. **B384** (1996) 123.
[35] H.P. Nilles and N. Polonsky, Nucl. Phys. **B484** (1997) 33.
[36] Models with two-loop neutrino masses from soft supersymmetry breaking tri-linear interactions were recently considered by F.M. Borzumati, G.R. Farrar, N. Polonsky, and S. Thomas, hep-ph/9902443, Nucl. Phys., in press.
[37] B. Barger, G.F. Giudice, and T. Han, Phys. Rev. **D40** (1989) 2987.
[38] G. Bhattacharyya, Nucl. Phys. Proc. Suppl. **52A** (1997) 83; hep-ph/9709395;
H. Dreiner, hep-ph/9707435;
R. Barbier *et al.*, *Report of the Group on the R-parity Violation*, hep-ph/9810232;
V. Bednyakov, A. Faessler, and S. Kovalenko, hep-ph/9904414.
[39] K. Agashe and M. Graesser, Phys. Rev. **D54** (1996) 4445.
[40] J. Erler, J. Feng, and N. Polonsky, Phys. Rev. Lett. **78** (1997) 3063.
[41] G. Bhattacharyya, J. Ellis, and K. Sridhar, Mod. Phys. Lett. **A10** (1995) 1699.
[42] J.-H. Jang, Y.G. Kim, and J.S. Lee, Phys. Lett. **B408** (1997) 367.
[43] L. Navarro, W. Porod, and J.W. Valle, hep-ph/9903474.
[44] S. Dimopoulos, R. Esmailzadeh, L.J. Hall, J.-P. Merlo, and G.D. Starkman, Phys. Rev. **D41** (1990) 2099;
J. Kalinowski, R. Ruckl, H. Spiesberger, and P.M. Zerwas, Phys. Lett. **B414** (1997) 297;
H. Dreiner, P. Richardson, and M. H. Seymour, hep-ph/9903419.
[45] In preparation.
[46] H. Dreiner and G. G. Ross, Nucl. Phys. **B365** (1991) 597.
[47] See, for example, S.I. Bityukov and N.V. Krasnikov, hep-ph/9712358.

[48] R.M. Godbole, P. Roy, and X. Tata, Nucl. Phys. **B401** (1993) 67.
[49] G.P. Lepage, J. Comp. Phys. 27 (1978) 192.